Mechanical and Structural Properties Underlying Contraction of Skeletal Muscle Fibers after Partial 1-Ethyl-3-[3-Dimethylamino)Propyl]Carbodiimide Cross-Linking

Sergey Bershitsky,* Andrey Tsaturyan,# Olga Bershitskaya,* Gregory Mashanov,* Paul Brown,§ Martin Webb,§ and Michael A. Ferenczi§

*Institute of Physiology, Urals Branch of the Russian Academy of Sciences, Yekaterinburg, Russia, #Institute of Mechanics, Lomonosov Moscow University, Moscow, Russia, and §National Institute for Medical Research, Mill Hill, London NW7 1AA, UK

ABSTRACT We show prolonged contraction of permeabilized muscle fibers of the frog during which structural order, as judged from low-angle x-ray diffraction, was preserved by means of partial cross-linking of the fibers using the zero-length cross-linker 1-ethyl-3-[3-dimethylamino)propyl]carbodiimide. Ten to twenty percent of the myosin cross-bridges were cross-linked, allowing the remaining 80–90% to cycle and generate force. These fibers displayed a well-preserved sarcomeric order and mechanical characteristics similar to those of intact muscle fibers. The intensity of the brightest meridional reflection at 14.5 nm, resulting from the projection of cross-bridges evenly spaced along the myofilament length, decreased by 60% as a relaxed fiber was deprived of ATP and entered the rigor state. Upon activation of a rigorized fiber by the addition of ATP, the intensity of this reflection returned to 97% of the relaxed value, suggesting that the overall orientation of cross-bridges in the active muscle was more perpendicular to the filament axis than in rigor. Following a small-amplitude length step applied to the active fibers, the reflection intensity decreased for both releases and stretches. In rigor, however, a small stretch increased the amplitude of the reflection by 35%. These findings show the close link between cross-bridge orientation and tension changes.

INTRODUCTION

The mechanical responses to sudden length changes observed in intact muscle fibers during contraction contain components described with rate constants as high as 2500 s^{-1} (Ford et al., 1977). The understanding of the structural changes that underlie these responses requires the development of techniques for the observation of structural change with sufficient time resolution. One successful technique for observing the molecular movement underlying muscle contraction is low-angle x-ray diffraction (see Huxley, 1996). The combination of whole muscle studies, synchrotron radiation, and fast electronic two-dimensional detectors (Bordas et al., 1991; Martin-Fernandez and Towns-Andrews, 1993) has allowed the study of many higher order reflections necessary for modeling of the cross-bridge structure. From the combination of the high resolution structure of the subfragment-1 fraction of myosin and its binding to thin filaments (Rayment et al., 1993a,b) and studies of the changes in the x-ray reflection pattern in contracting muscle, a detailed understanding of the cross-bridge movement during energy transduction emerges (see Squire and Harford, 1993). A time resolution of 1 ms was achieved by Huxley et al. (1983) in x-ray diffraction experiments on whole frog muscles where fast molecular movements following sudden length changes were observed. In single

muscle fibers, a time resolution of 0.1 ms in the measurement of changes in the 14.5-nm meridional x-ray reflection (Irving et al., 1992; Lombardi et al., 1995) allowed the discrimination of the passive elastic responses from the "power stroke," the active response of the muscle cross-bridges responsible for force production.

These results have been obtained in intact muscles or muscle fibers, where the cellular homeostatic mechanisms maintain and control the chemical environment of contractile proteins. Much would be gained, however, by experiments in which the time course of the brightest x-ray reflections could be measured in permeabilized skeletal muscle fibers from the frog where the environment of the muscle proteins can be manipulated to investigate the correlation between chemical, mechanical, and structural changes.

In permeabilized frog muscle fibers, preservation of the sarcomere structure during activation is difficult, even at low temperature (Goldman and Simmons, 1984, 1986). The loss of sarcomere structure is accompanied by a deterioration of the mechanical responses to imposed length changes and by loss of features in the x-ray diffraction. The relatively slow diffusion of calcium into the center of muscle fibers during activation results in nonhomogeneous activation and disruption of the structure. The high shortening velocity and the large diameter of frog fibers aggravate the activation damage compared with permeabilized muscle fibers of the rabbit at low temperature where the order of the sarcomeres and of the equatorial x-ray reflections have been successfully preserved (Brenner and Yu, 1993). Even in these fibers, however, disordering occurs at higher (>15°C) temperatures, where the shortening velocity approaches that

found in frog muscle fibers at low temperature. Temperature below 15°C is not physiological for rabbit muscle fibers. The meridional x-ray reflections arising from the axial repeat of the cross-bridges are particularly weak in rabbit muscle at low temperature compared with the equatorial reflections (Wray, 1987).

Frog muscle fibers do, however, benefit from certain advantages over rabbit muscle fibers and whole frog muscles. Frog fibers are larger than rabbit fibers (approximately twice the diameter), which results in greater x-ray diffraction power, and, in effect, better signal/noise ratio. The mechanical characteristics and x-ray diffraction features of intact frog muscle fibers are well documented. Single muscle fibers as opposed to whole muscles were used (Huxley et al., 1983) because of the ability to permeabilize single cells reliably and, therefore, control the chemical environment of the myofibrils. Also, the changes in sarcomere length can be measured with more precision for single fibers than for whole muscles.

We describe below a method that maintains the structure and mechanical characteristics of permeabilized frog muscle fibers during active tension development. This method involves the use of partial cross-linking of the myofilaments using the zero-length cross-linker 1-ethyl-3-[3-dimethyl-amino)propyl]carbodiimide (EDC) (Tawada and Kimura, 1986) to stabilize the muscle fiber structure during force development. On the basis of stiffness measurements, we determined that in the experiments shown here, 80–90% of the myosin cross-bridges are unaffected by the cross-linking procedure.

Measurements are shown of the intensity of the main meridional and equatorial reflections obtained for permeabilized frog muscle fibers in the relaxed, rigor, and active states. The x-ray diffraction patterns from these fibers were close to those found in intact muscles and muscle fibers during relaxation and activation. Also, changes in the x-ray

diffraction characteristics for the rigor state were reversible and therefore arose from a change in the cross-bridges, not from the loss of the structural order. Changes in the intensity of the 14.5-nm meridional reflection induced by length changes were used as a probe of cross-bridge orientation (Irving et al., 1992). The measurements were obtained with a time resolution of 2 ms, comparable with the speed of cross-bridge movement as deduced from mechanical measurements and from x-ray diffraction. Assuming that there was no detachment and attachment of cross-bridges, changes in intensity of the 14.5-nm reflection could be caused by a change of orientation of the whole myosin cross-bridge in the plane parallel to the fiber axis, or by a change in angle between the catalytic domain and the light-chain tail of myosin subfragment-1. The experiments described here, however, could not distinguish between these latter possibilities as measurements of weaker reflections corresponding to higher orders of the 14.5-nm repeat would be necessary. X-ray diffraction was observed while the muscle fibers were suspended in air, as this decreased the background scatter in the recordings. This procedure was evaluated.

MATERIALS AND METHODS

Muscle fibers

Bundles of muscle fibers from the semitendinosus muscle of *Rana temporaria* were placed in a dissecting dish containing relaxing solution (Table 1) at 8–12°C and cooled to 2–4°C. Five- to six-mm-long segments of single fibers were teased out and installed on the experimental set up. The attachment of the fiber ends to the apparatus was carried out with the fiber immersed in a drop of relaxing solution on a piece of cover-glass. The ends of the muscle fibers were attached to the nickel tube of the motor moving part and to the nickel tube of the tension transducer. The attachment was carried out at 5°C. The muscle ends were glued in place using shellac dissolved in ethanol to a thick paste consistency (Bershitsky and Tsaturyan, 1989, 1992). After attachment, the cover glass was removed and the fiber

TABLE 1 Composition of the experimental solutions (mM)

	Relaxing −CP	Relaxing +CP	Activating	Prerigor	BDM rigor	Rigor	Cross-linking	Super-Relaxing
MOPS	100	100	100	100	100	100	–	–
ATP	5	5	5	0.5	–	–	–	5
Mg Acetate	6.5	6.5	6.5	2	–	–	–	6.5
CP	–	35	32	–	–	–	–	25
EGTA	5	5	–	5	–	–	–	5
CaEGTA	–	–	5	–	–	–	–	–
EDTA	–	–	–	–	5	5	–	–
KPr	70	–	–	80	85	85	–	–
K₂HPO₄ + KH₂PO₄	–	–	–	–	–	–	50	50
BDM	–	–	–	5	3	–	–	50
EDC	–	–	–	–	–	–	10	–
CK (mg · ml⁻¹)	–	2.5–3	2.5–3	–	–	–	–	2.5–3

The ionic strength of the solutions was ~0.2 M, calculated using the stability constants and temperature coefficients given by Godt and Lindley (1982). For MOPS, pK and temperature coefficient were obtained from the manufacturer.

MOPS, 3-[*N*-Morpholino]propanesulfonic acid; ATP, adenosine 5'-triphosphate, disodium salt; CP, creatine phosphate, disodium salt; EGTA, ethylene-glycol-*bis*-(β-aminoethyl ether)-*N,N,N',N'*-tetraacetic acid; EDTA, ethylenediaminetetraacetic acid; KPr, potassium propionate; BDM, 2,3 butanedione monoxime; EDC, 1-(3-Dimethyl-aminopropyl)-3-ethyylcarbodiimide; CK, creatine kinase.
All chemicals except CK were from Sigma Chemical Co.

segment, 3.2 ± 0.5 mm in length, was placed in the solution by raising the moving chamber. The sarcomere length of the muscle fiber was adjusted to 2.05–2.15 μm using the position of the first-order diffraction line generated by diffraction of a 5-mW He-Ne laser beam. The fiber dimensions were measured in two perpendicular directions.

Permeabilization

Two methods of permeabilization were used. One was to immerse single fibers in 0.5% Triton X-100 in relaxing solution in a dissecting dish (Table 1) for 15–30 min at 5–10°C immediately before mounting them in the experimental chamber. In some cases fibers were additionally treated with glycerol. For this, they were immersed in 25% (v/v) glycerol in relaxing solution for 15 min, then in 50% (v/v) glycerol for 15 min, and finally transferred into the relaxing solution. This procedure resulted in an improvement in permeabilization as judged from the reduction of time taken for the fibers to reach a rigor state (see below), with no deterioration in the x-ray diffraction pattern.

The second method of permeabilization was a 10-min exposure to relaxing solution containing 20 unit·ml^{-1} of purified α-toxin at 20°C (Nishiye et al., 1993). After α-toxin treatment, the temperature in the trough was lowered to 0°C.

Rigorization

The way in which muscle fibers were rigorized was found to be critical to the preservation of fiber sarcomere order and that of the x-ray diffraction pattern. At 0–1°C, the relaxing solution bathing a muscle fiber was changed to one containing 0.5 mM ATP and 5 mM 2,3-butanedione monoxime (BDM, "pre-rigor" solution). After a 5- to 10-min incubation, the temperature was increased to 10°C for 10 min to accelerate ATP depletion and lowered again to 0°C, and the solution was exchanged for rigor solution (Table 1) containing 3 mM BDM. The onset of rigor was tested by measuring the force response to the application of small amplitude stretches (0.1–0.2% of the fiber length). When stiffness began to appear ($S \geq 5$ MN·m^{-2}; where the stiffness $S = \Delta Tl/\Delta l$, l is the length of a half-sarcomere, and Δl and ΔT are changes of l and of tension, T), the temperature was gradually increased to 10–15°C to accelerate ATP utilization and to establish full rigor stiffness. After that, temperature was returned to 0°C and the chamber was filled with EDTA rigor solution. Typically, the total procedure took 40–60 min. Under these conditions, no spontaneous tension rise was observed and the total brightness of the first-order line of laser diffraction never decreased by >30% of its value in the relaxed fiber. Usually, the brightness decrease resulted from a change in the Bragg angle and could be restored by changing the angle of the incident beam. The width of the first-order diffraction line was normally unchanged at this stage.

EDC cross-linking

The procedure is based on that developed by Tawada and Kimura (1986). After stabilization of the fiber's rigor state, the muscle fiber was washed with 50 mM phosphate buffer and incubated at 15°C in 10 mM EDC in the same buffer for 9–11 min (Bershitsky and Tsaturyan, 1995a). The temperature was then decreased to 5°C, and the chamber was washed twice with 50 mM phosphate buffer to remove any remaining EDC then filled with rigor solution. Freshly prepared solutions of EDC were essential to achieve reproducibility of the extent of cross-linking. The extent of cross-linking was estimated as the stiffness in a "super-relaxing" solution (see below) normalized for that in rigor.

Experimental solutions

The experimental solutions used are shown in Table 1. The activating solution contained 2.5–3 mg/ml muscle creatine kinase (CK), which was

either purchased from Sigma Ltd. (Poole, Dorset) or purified in the laboratory from chicken breast muscle as described below. The creatine kinase activity of the enzyme purified in the laboratory was two to three times greater (>320 unit·mg^{-1} at 25°C, pH 7.0) than the commercial product, and its use was found to improve the maintenance of the activated state during our experiments.

Preparation of creatine kinase from chicken muscle

All procedures were carried out in the cold. Breast muscle (260 g) was removed from a fresh chicken from a supermarket. The muscle was minced and homogenized with twice its volume of 10 mM KCl, plus 0.1 mM EDTA. After ~5 min, the mixture was centrifuged at 8000 rpm for 20 min and the supernatant was filtered through Whatman No. 1 filter paper, using suction. After adjusting the pH to 8.0 with Tris base, the solution was dialyzed against 10 mM Tris·HCl, pH 8.0, 0.1 mM EDTA for 24 h, with occasional mixing and with a change of buffer. A Q-Sepharose column (100 ml) was preequilibrated in 10 mM Tris·HCl, pH 8.0, and the protein solution was fractionated on this column after dilution to give the same conductivity as the preequilibration buffer. Protein was eluted with a gradient (2 l) from 0 to 90 mM KCl in 10 mM Tris, pH 8.0. Fractions were monitored by SDS-PAGE and by enzyme activity assays (see below). Fractions containing creatine kinase at >90% purity were pooled, concentrated to >10 mg·ml^{-1} using an Amicon concentrator and stored in aliquots at −80°C. (For some measurements, the protein was further purified on Sephadex G150 gel filtration medium (2.5 cm × 70 cm) in 50 mM Tris·HCl, pH 7.5, 100 mM KCl, and run at 0.4 ml·min^{-1}). The protein had a specific activity of 338 unit·mg^{-1}. By comparison rabbit muscle creatine kinase (Sigma Ltd., Poole, Dorset, 250 unit·mg^{-1} as assayed by Sigma at pH 7.4, 30°C) was 104 unit·mg^{-1}, mainly due to lower protein purity: the rabbit protein showed three major bands on SDS-PAGE.

Creatine kinase assay

The assay solution (1 ml) was as follows in 50 mM PIPES, pH 7.0: 5 mM MgCl$_2$, 5 mM creatine phosphate, 1 mM ADP, 1 mg·ml^{-1} glucose, 1 mM NAD, 10 unit·ml^{-1} hexokinase (from yeast), 10 unit·ml^{-1} glucose-6-phosphate dehydrogenase (from Leuconostoc mesenteroides). The reaction at 25°C was initiated by addition of ~0.025 unit creatine kinase and monitored by absorbance at 340 nm. The coupling enzymes were obtained from Sigma as lyophilized solids free of sulfate and were stored at −80°C as solutions in water at 1000 unit·ml^{-1}. The concentration of creatine kinase was calculated using a theoretical absorbance of 0.767 for a 1 mg·mL^{-1} solution (Gill and von Hippel, 1989), which is the same for rabbit and chicken muscle enzymes. The assay was unaffected by the use of MOPS buffer instead of PIPES.

The experimental chamber

The experimental chamber is shown in diagrammatic form (Fig. 1). A muscle fiber was immersed in the trough by attaching its ends to the tension transducer and motor as described above. The muscle fiber was either immersed in the experimental solution (upper position) or was suspended in air (trough in lower position, as shown). The fiber's environment (in or out of the trough) was set remotely by means of a motorized drive, controlled from outside the interlocked x-ray experimental area. The movement of the trough was complete in less than 2 s. The muscle fiber was exposed to air 1–3 s before the opening of the x-ray shutter, and immediately returned to the experimental solution at the end of the exposure to x-rays, usually 2–3 s later.

Measurements carried out while the muscle fiber was suspended in air offered the following advantages: 1) The need for x-ray transparent windows was avoided. Although mica or kapton windows have sometimes been used, their x-ray absorption and the gradual accumulation of dirt results in attenuation and deterioration of the x-ray signal. 2) The need for
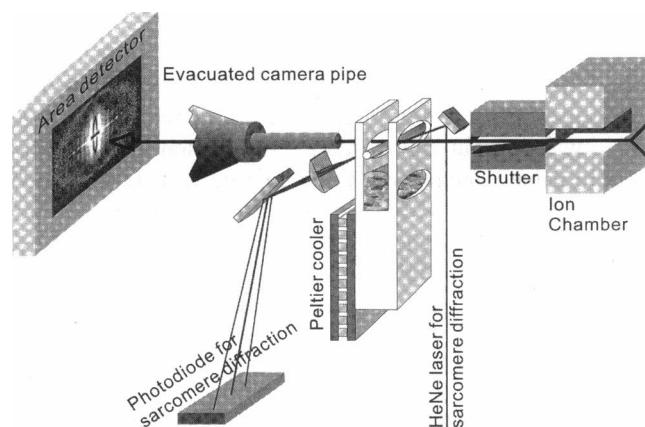
FIGURE 1   Diagrammatic representation of the experimental system (not to scale). The muscle fiber is shown suspended in air. The motor and tension transducer holding the fiber and the motor used for moving the trough up and down are not shown, for clarity. The x-ray beam is traveling horizontally from right to left.

a constant thickness of water in the chamber surrounding the fiber in the x-ray path was avoided. Such a water layer, often necessarily several times the thickness of the muscle fiber, also contributed to attenuation of the diffraction signal. Potential disadvantages of measurements while the muscle fiber was suspended in air were that the temperature of the fiber in air was more difficult to measure and control, water evaporation may have resulted in a change in the physicochemical characteristics of the muscle fibers, and the lack of diffusion and equilibration of chemicals in the muscle fiber with the bathing solution imposed constraints on the practical duration of the experiment. Here, the cooled experimental chamber that surrounded the fiber while it was suspended in air (Fig. 1) was designed specifically so that the fiber temperature was maintained at 5–6°C, well below the condensation temperature, thus avoiding evaporation. An evaluation of the consequences of measurements carried out while the muscle fiber was suspended in air is given in the Results section.

When the fiber was bathed in the experimental solution, the x-ray beam and that of the 5 mW He-Ne laser used for measuring the sarcomere signal passed through two mica windows (<5 μm). When the fiber was suspended in air, there was no x-ray scatter or attenuation caused by the chamber solution or windows. The volume of the solution-containing part of the trough was 140 μl, including 30 μl in the tubing used for emptying and filling of the trough. The gap between the trough windows was 1.5 mm. The air gap between the synchrotron window and the nose cone window on the camera was 11 cm, 3.5 cm resulting from the ion chamber used for monitoring the incident x-ray beam intensity and 5 cm resulting from the fast shutter (NM Laser Products, Inc., CA) used in these experiments. The air gap between the fiber and the nose cone of the evacuated camera pipe was 1.5 to 2 cm, which minimized scattering of the diffraction peaks. The trough temperature was adjusted by a remotely-controlled Peltier element affixed to the outer-wall of the chamber. Important considerations in the design of the chamber were to ensure that the fiber temperature did not vary while suspended in air and to ensure that no evaporation took place. When suspended in air, the fiber environment was kept cold and moist by the surrounding aluminum. When the solution temperature was set at 0°C, the temperature of the fiber in air was 5°C and remained constant for ~30 s. The fiber suspended in air scattered diffracted laser light. For this reason one of the first-order diffraction peaks was focused on the position sensitive photodiode (LSC/30D; United Detector Technology, Hawthorne, CA) with a cylindrical lens. Changes in sarcomere length were monitored as described by Bershitsky and Tsaturyan (1995b). Some variation in the optical properties was caused by a slight variation in the fiber shape and the amount of solution accompanying the fiber each time it passed through the solution/air interface.

The motor for changing fiber length

The stator of a loud-speaker type motor was made from Nd-Fe-B magnets (Institute of Physics of Metals, Urals Branch of the Russian Academy of Sciences, Yekaterinburg, Russia). The moving part of the motor was made from thin-wall catalin (Catalin Ltd., Essex, UK) tube, $\varnothing$ 3 mm and 15 mm long, reinforced by strips of carbon fiber sheet (Goodfellows, Cambridge, UK). At the rear end of the moving part was a coil, 8.5 mm in diameter, made of 25 turns of $\varnothing$ 0.14 mm copper wire. The front end was terminated by a half-cut nickel tube, $\varnothing$ 0.35 mm (Goodfellows, Cambridge, UK), at the end of which the muscle fibers were glued. The moving part was suspended on two flexible membranes made from 0.1-mm-thick phosphor bronze. A flag-type position sensor consisting of a 6-mW infrared light-emitting diode (AL-107, Russia) and a twin photodiode (FD-20-30K, Russia) had noise corresponding to 0.05 μm peak-to peak and a linear range of $\pm$200 μm. The motor was assembled in a $\varnothing$ 30 mm $\times$ 50 mm aluminum cylinder. The motor permitted step displacements up to $\pm$50 μm within 0.14 ms.

Tension transducer

A piezo-electric force transducer was used (Bershitsky and Tsaturyan, 1992, 1995b). It had a resonant frequency of 15–20 kHz and a time constant of electric charge drain of $\geq$10 s. The transducer noise corresponded to <5 μN. A shortening step of 2–4% of the fiber length (slack test) was applied to each muscle fiber at the end of each record to measure the tension baseline.

Control of experiments and data acquisition

Displacement of the length step motor was controlled using a DAC card (L-154, L-Card, Moscow, Russia) and was synchronized with the x-ray framing. Force, fiber length, and sarcomere length changes were recorded using a four-channel, high-speed, data-acquisition interface (DAS-50; Keithley MetraByte Corp., Taunton, MA), with data collection frequency usually set at 50 kHz/channel. Both L-154 and DAS-50 cards were installed in a PC and controlled the experimental conditions during data acquisition. Software for exponential analysis was Scientific Graphic Interactive Management System (GIM, Versions 3.0; © by A. Drachev).

Modeling of intensities of x-ray reflections

Mathematical modeling of intensities of the strongest equatorial reflections (1,0), (1,1) was made using the model proposed by Malinchik and Yu (1995).

X-ray collection and analysis

The data were collected on beam lines 2.1 and 16.1 at the Synchrotron Radiation Source in Daresbury, using the two-dimensional, wire-chamber-type, electronic area detectors No. 6 and 5, which have a collection area of ~20 $\times$ 20 cm (Towns-Andrews et al., 1989). After diffraction and scatter by the fiber, the x-ray beam of a nominal wavelength of 0.154 nm (beam line 2.1) or 0.141 nm (beam line 16.1) traveled through the entrance mica window of an evacuated beam-pipe and through a Mylar window at the detector end. The nondiffracted beam (direct beam) was attenuated by a nontransparent (beam line 16.1) or semitransparent beam stop (0.35-mm-thick Ni, beam line 2.1) placed in the beam pipe near the detector. The x-ray beam was focused horizontally at the detector to provide the sharpest meridional reflections, but was focused vertically at the fiber to maximize x-ray flux at the sample. The total fiber-detector distance was 2.79 m on beam line 2.1 and 4.1 m on beam line 16.1. The x-ray data were collected on the station's VME computer at a sampling frequency of 1 kHz during the rapidly changing phases of the observed transients, before transfer to the laboratory's UNIX workstation for analysis. The images were usually

collected by operating the detector to obtain an image of 256 × 256 pixels for each time frame. Some experiments were carried out with 512 × 512 pixel resolution. The analysis was carried out using the suite of programs, chiefly BSL and XOTOKO, provided by the Collaborative Computing Project (CCP13) of the Engineering and Physical Sciences Research Council. The data were corrected for detector nonlinearity using a calibration with Fe[55] radiation and corrected for camera scatter by subtraction of a camera blank image. The four symmetrical quadrants were summed. Rotation of the diffraction pattern before summing of the four quadrants was usually not necessary, as in most cases the horizontal alignment of the fibers was adequate. The equatorial and meridional intensities were calculated after reduction of the two-dimensional images to one-dimensional scans. This was achieved by summing the counts in bands along the equator and the meridian. The width of the bands were selected by eye to include all the photons in the main reflections. The intensity of the x-ray reflections for the main reflection peaks was calculated after subtraction of the background scatter caused by the fiber. This was achieved by linear interpolation of the background signal under each peak. For short time frames, the background signal was time-averaged before subtraction, with weighting to take into account the variation in data collection time for individual time frames in each sequence. This averaging minimized the increase in noise in the signal resulting from the subtraction of noisy background from noisy peak data. This procedure assumed that the background signal under each peak changed little compared to the change in the peaks themselves during the data collection period.

RESULTS

Muscle fibers in air

Most of the measurements were carried out while the muscle fibers were suspended in air. As found previously by others (Poole et al., 1988; Ferenczi et al., 1984), we also found that x-ray diffraction and mechanical properties of muscle fibers were well maintained in spite of exposures of a few seconds in air (see below). The atmosphere surrounding the muscle fibers was set at a temperature well below the condensation temperature (5–6°C) so that the fibers remained moist throughout. This was achieved by means of the cooled metal surrounding the fiber (Fig. 1). A temperature probe placed in the fiber position showed that the temperature remained at <6°C for the first 30 s of exposure to air. The exposure to air of muscle fibers was limited to periods of <10 s. In the case of activated muscle fibers, this period was never >4 s, as the high ATPase activity during activation resulted in the eventual depletion of ATP and accumulation of ADP and creatine, even in the presence of the ATP regenerating system as evidenced by a slowing down of the force responses to induced length changes.

Mechanical properties of muscle fibers in rigor

At 0–1°C in the presence of 3 mM BDM, rigorization was slow. Stiffness reached 5 MN·m^{-2} or ~15-20% of its rigor value in up to 30 min. The temperature was increased gradually in 5°C-steps to 10–15°C to accelerate ATP splitting and stiffness development while avoiding any significant tension rise. The intensity and width of the first-order diffraction maximum of the He-Ne laser beam did not change significantly during the rigorization, showing that the sarcomere structure remained ordered during this pro-

cedure. Despite the low tension (≤30 kN·m^{-2}), full rigor stiffness (usually > 30 MN·m^{-2}, although in some fibers with low tension, stiffness reached ~20 MN·m^{-2}) eventually developed in the presence of BDM (*Trace 1* in Fig. 2). After washing out BDM (*trace 2*), rigor tension and stiffness remained unchanged. Cross-linking with 10 mM EDC for ~10 min at 15°C did not affect rigor tension and rigor stiffness significantly (*trace 3*). In rigor, muscle fibers were almost purely elastic. Tension changed instantaneously with sarcomere length and tension relaxation was small and slow (see Fig. 2).

Mechanical properties of the muscle fibers after EDC cross-linking

After EDC cross-linking, fibers were immersed for 20–30 min at 0–2°C in relaxing solution containing 35 mM creatine phosphate and 2.5–3 mg·ml^{-1} CK to allow CK to diffuse into the fiber. Relaxing solution was replaced by activating solution and fibers developed isometric tension of 80–120 kN·m^{-2}. The stiffness of the fiber in activating solution was 65–70% of that in rigor. During activation, the intensity of the first-order laser diffraction peak did not decrease by more than 30%. Tension and the laser diffraction pattern remained practically constant for 2 h or more of continuous activation. Experiments were ended when tension reached 85% of the initial value. The drop in tension was caused by repeated transfer of the fibers through the air/water interface in the course of the experiment, and not by a gradual decline in the isometric tension developed by the undisturbed fiber. Partial EDC cross-linking, therefore,
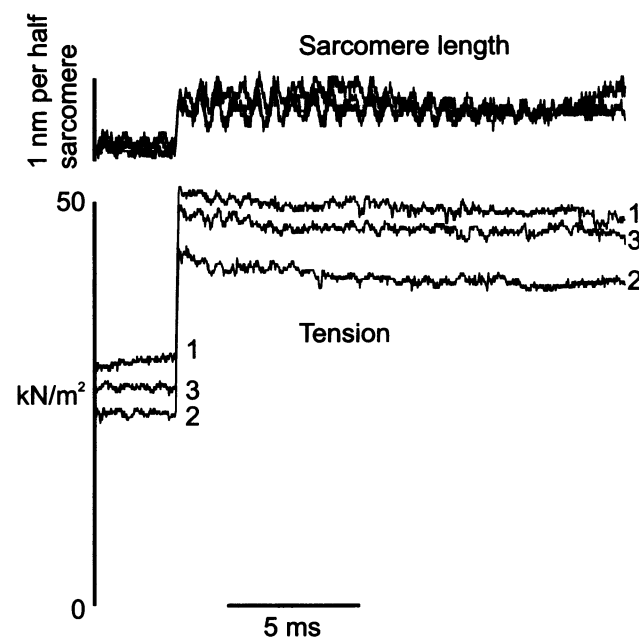

FIGURE 2   Tension in rigor solutions. Sarcomere length (*upper traces*) and tension (*lower traces*) responses to step stretches of a fiber. *1*: BDM-rigor; *2*: rigor before cross-linking; *3*: rigor after EDC cross-linking. Fiber dimensions: 3.67 mm × 15710 μm^2; sarcomere length: 2.1 μm; 5°C.

protected the sarcomere structure from disordering even when substantial force was developed. Fibers treated with EDC did not shorten by >3%, as some actin-myosin bonds were covalently cross-linked. When shortening steps of 2.5% of the muscle length were applied, some tension development followed, indicating that partially cross-linked fibers could still shorten somewhat beyond that length. With 3% steps, no further tension development was seen. However after small length steps, the elastic tension response was followed by the fast partial tension recovery (Fig. 3) as described by Huxley and Simmons (1971) for intact muscle fibers. The rate constant of the fast tension recovery (Huxley-Simmons phase 2) after fiber shortening by 2–3 nm per half-sarcomere ($1300-1700$ s^{-1}) was close to that found in intact muscle fibers ($1500-2500$ s^{-1}; Ford et al., 1977). When fibers were suspended in air for 2–4 s, tension increased by 10–20% as temperature increased from $0-2°C$ to $5-6°C$. The ability of fibers to produce the fast partial tension recovery characteristic of intact fibers while suspended in air depended on the efficiency of the ATP backup system. Up to 3 mg·ml^{-1} of commercial rabbit CK resulted in a rate constant for the fast tension recovery of ≤ 500 s^{-1}, i.e., significantly less than seen in intact fibers. The same concentration of chicken CK prepared in the laboratory maintained a rate constant of $1300-1700$ s^{-1} for as long as 4 s (Fig. 3). If the fiber remained in air longer than this, mechanical transients slowed down.
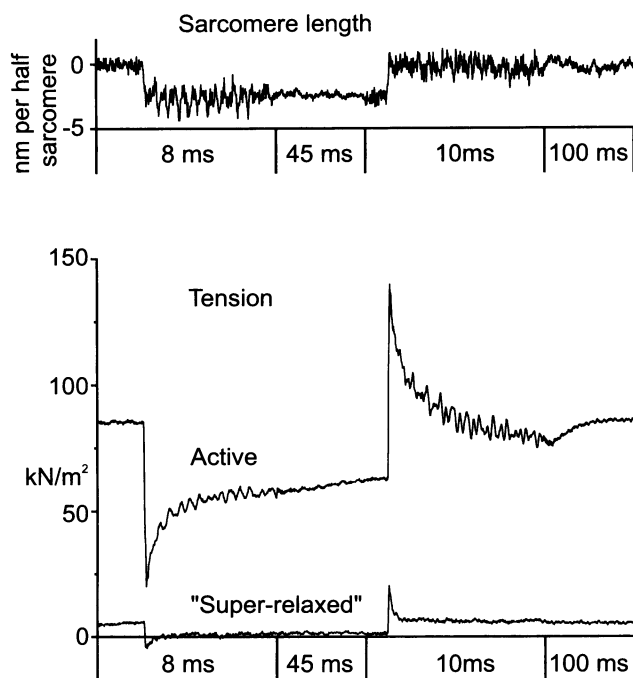

FIGURE 3 Mechanical responses to step length changes of a fiber suspended in air for 2 s. The fiber had been cross-linked with 10 mM EDC for 10 min at 15°C. The fiber was immersed in activating or super-relaxing solution before being suspended in air. The sarcomere record (*upper trace*) is shown only for the activated fiber as in super-relaxing solution, the fiber was slack following the release and the sarcomere signal was noisy. Same fiber as in Fig. 2, 5°C.

Estimation of the extent of EDC cross-linking

In relaxing solution of 0.2 M ionic strength, cross-linked fibers produced a tension $\sim 50\%$ of that in activating solution. Stiffness was also about half its active value. However tension and stiffness in the absence of Ca^{2+} were only partially caused by the cross-linked myosin cross-bridges. Unlinked myosin cross-bridges most probably also participated in the mechanical responses in the conventional relaxing solution, because EDC was shown to cross-link components of actin-tropomyosin-troponin complex (Grabarek and Gergely, 1990; Leszyk et al., 1990) and the cross-linked myosin cross-bridges probably switched on the regulatory proteins (Tawada and Kimura, 1986; Bershitsky and Tsaturyan, 1995b). Unlinked myosin cross-bridges detached from the thin filaments by increasing the ionic strength of the relaxing solution to 0.6–2 M (Tawada et al., 1989). It was shown by Tawada and Kimura (1986) that high salt concentration did not induce solubilization of the backbone of the thick filaments as they were also cross-linked with EDC. However the spacing of the (1,0) and (1,1) equatorial x-ray reflections increased markedly at high ionic strength making it difficult to interpret the x-ray data. We used instead a super-relaxing solution with an ionic strength of ~ 0.2 M (Table 1), which contained 50 mM BDM and 50 mM inorganic phosphate (P_i). This maximally decreased tension and stiffness of EDC treated fibers. It is likely that this resulted from the detachment of the cross-bridges, which were not cross-linked to the thin filaments. Fig. 3 shows tension responses to step length changes in a fiber suspended in air after it was immersed in activating and super-relaxing solutions. In the super-relaxing solution, the fiber still produced fast tension transients, but tension and stiffness were low ($<10\%$ and 12–20%, respectively) compared to active contraction showing that only a fraction of the cross-bridges were cross-linked and could not detach from the thin filaments.

Huxley-Simmons transients in partially cross-linked fibers

Sudden length step changes of $+3$ (stretches) to -7 nm (releases) per half-sarcomere were applied to the partially cross-linked fibers immersed in activating solution (Fig. 4) (monitoring of the sarcomere length was easier than in air). Tensions at the end of the length step (T_1), and at the end of the fast (T_2) and slow (T_4) phases of tension recovery were normalized for isometric tension (T_0) and plotted in Fig. 5 A against the step size. Strain dependence of the rate constant (k_2) of the fast partial tension recovery is shown in Fig. 5 B. The amplitudes and kinetics of the mechanical transients were similar to those in intact muscle fibers (Ford et al., 1977). The main difference was the incomplete tension recovery caused most probably by cross-linked myosin cross-bridges that could not reattach to new actin sites and resisted the length change.
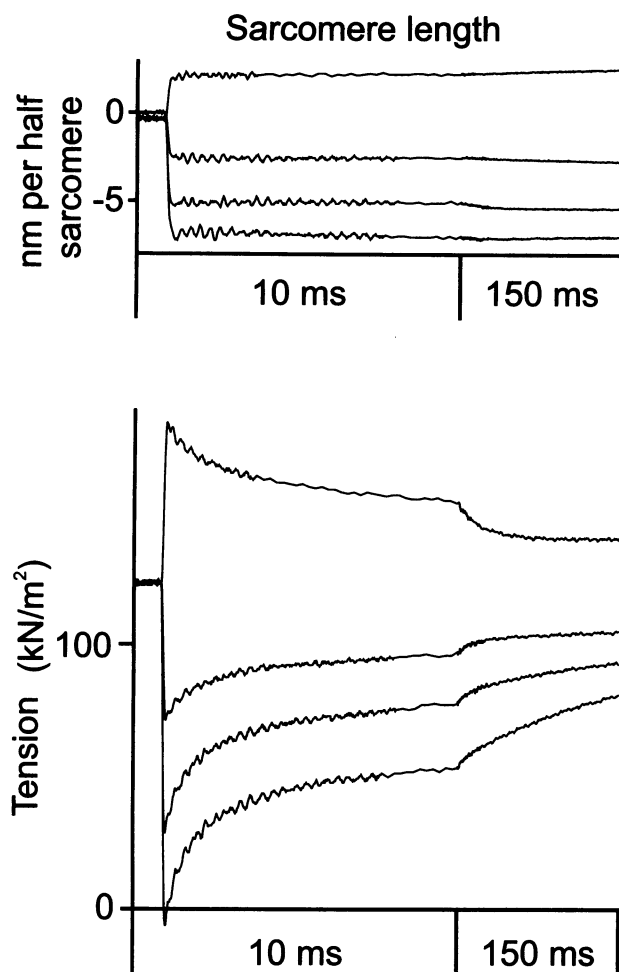
Sarcomere length

FIGURE 4 Mechanical transients in a slightly cross-linked fiber in activating solution at 0°C. Sarcomere length (*upper traces*) and tension (*lower traces*) after step length changes. Fiber dimensions: 2.28 mm × 5770 μm^2; sarcomere length; 2.15 μm; 1°C.

FIGURE 5 *A*: Tension at the end of the length step (T_1), at the end of the fast partial tension recovery (T_2), and at the plateau of the slow tension recovery (T_4) normalized for isometric tension (T_0) are plotted against the step size (*y*) for the mechanical transients shown in Fig. 4. Two points of the T_1 curve in super-relaxing solution are shown after normalization for T_0 to estimate the proportion of cross-linked myosin cross-bridges. *B*: Dependence of the rate constant of the fast partial recovery (k_2) on the step size. Squares represent the experiment shown in Fig. 4, pentagons refer to a second fiber.

The x-ray diffraction pattern

The x-ray diffraction pattern obtained from muscle fibers suspended in air was found to differ from that of fibers immersed in experimental solutions only in that in the latter case, the x-ray beam was attenuated and scattered by the water. For fibers suspended in air, the x-ray data were corrected for camera scatter by subtraction of the x-ray signal obtained through the air gap. In the case of fibers immersed in experimental solution, the x-ray data were corrected for camera scatter by subtraction of the x-ray signal obtained through the solution-filled chamber. This meant that fibers were replaced by the same thickness of water in the background signal, whereas in the former case, the fiber water was not subtracted. Scaling the pattern obtained in the solution chamber (1.5-mm-thick) by a factor of 4–6 resulted in a pattern close to that obtained with the fiber suspended in air, both for the meridian and for the equator, except for the higher noise level due to the attenuation of the beam through the water-filled chamber.
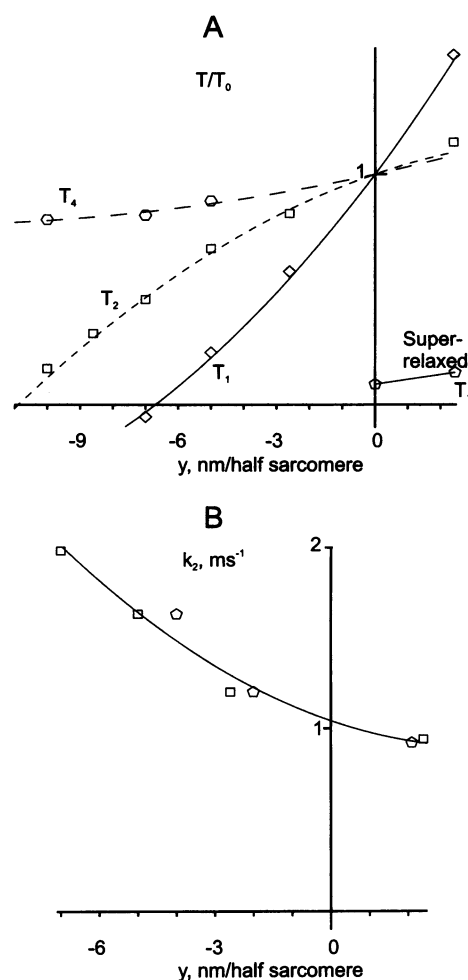
The x-ray diffraction pattern of a muscle fiber in air at 5°C is shown in Fig. 6, following 10-s exposure of the relaxed fiber before EDC cross-linking (top left quadrants), 10-s exposure of the fiber in rigor after slight EDC cross-linking (top right quadrants), and 6-s exposure of the activated fiber (bottom halves of each pattern) obtained in 60 0.1-s exposures in air interspersed with periods in activating solution. The two panels of the figure show different levels of contouring. The rigor pattern before cross-linking was very similar to that after cross-linking (pattern not shown, see Table 2). The striking feature of the patterns was the presence of strong inner layer lines in the relaxed pattern, which, in the rigor pattern, were replaced by a set of layer lines further from the meridian. During active contraction, the intensities of the actin layer lines decreased markedly compared to those in rigor. The layer lines in the active
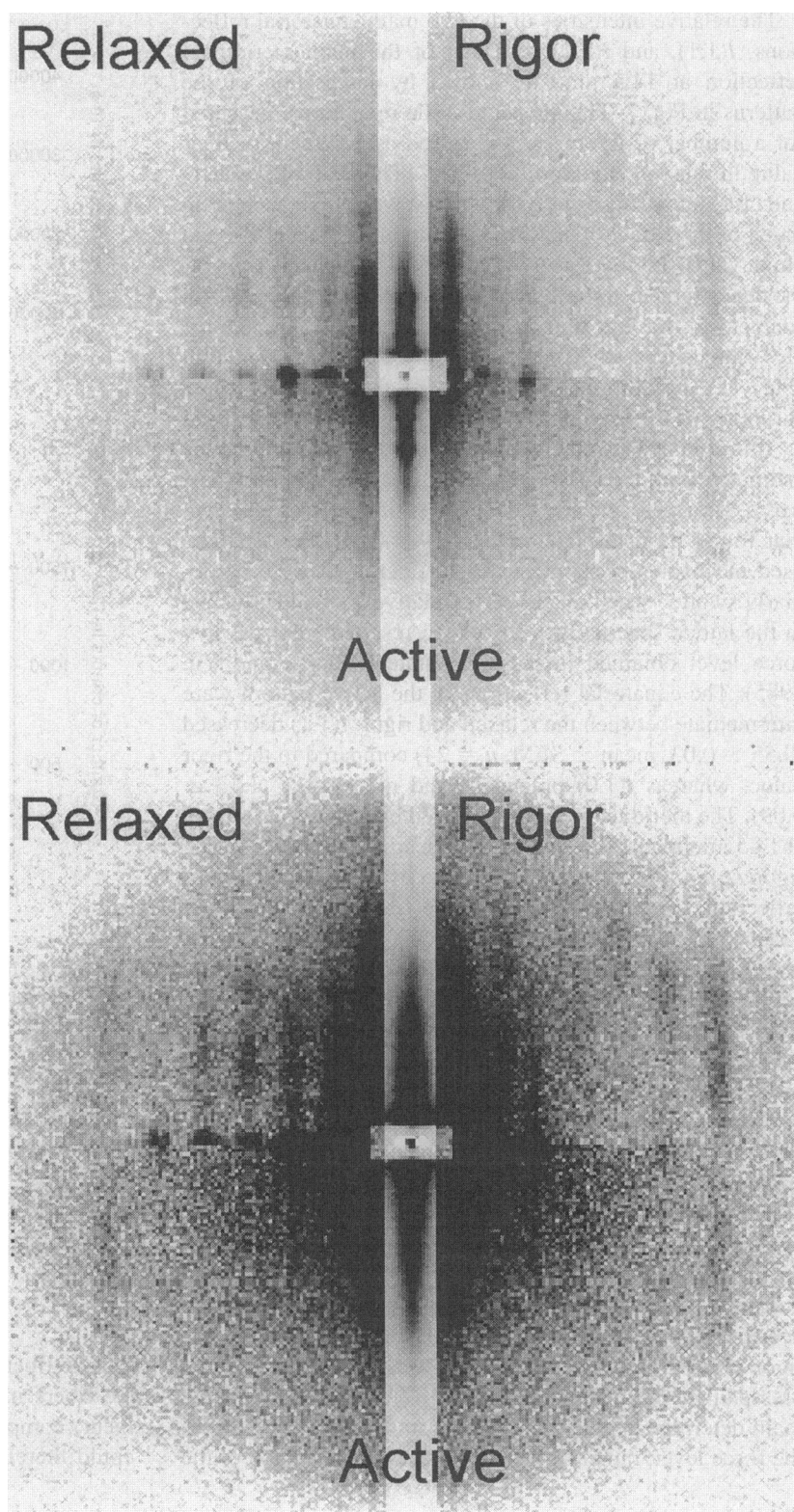
FIGURE 6 Diffraction patterns obtained from a single muscle fiber of frog semitendinosus muscle at 5°C on beam line 2.1. The patterns on the top and bottom are identical except for the contouring levels, which differ by a factor of 4. The orientation of the pattern is as collected with muscle fibers held horizontally; the equator is vertical. The top left quadrant of each figure was obtained with a 10-s exposure of the relaxed fiber after permeabilization with Triton X-100. The top right quadrant was a 10 s exposure of the muscle fiber in rigor after EDC cross-linking. The bottom half of each figure was obtained during activation. The active pattern is the result of 6-s exposure of the muscle fiber achieved by summing sixty 0.1 s exposures with the muscle fiber suspended in air, interspersed with intervals in activating solution for re-equilibration of the experimental solution. The active pattern was scaled by 1.67 to match the exposure of the relaxed and rigor patterns. The rigor and active patterns were additionally scaled by 1.04 and 1.1, respectively to account for the decay in the intensity of the synchrotron beam during the experiment. A strip along the equator was attenuated by a factor of 20 for display. Fiber dimensions: 3.06 mm × 13900 μm^2, sarcomere length: 2.15 μm.

pattern obtained here appear slightly brighter than those seen in contraction of intact muscles (Huxley et al., 1982). Quantification of the layer line intensities is difficult, but we cannot exclude the possibility that the intensification of the actin layer lines by myosin cross-bridges is enhanced more by cross-linked myosin cross-bridges than by normally cycling cross-bridges.

The most pronounced layer line in the active pattern, which is slightly more intense than in the relaxed muscle, is the 5.9-nm layer line (Huxley and Brown, 1967).

The relative intensities of the two main equatorial reflections, $I(1,1)$, and $I(1,0)$, and that of the main meridional reflection at 14.5 nm, are shown by integration of the patterns in Fig. 7. The intensity of the reflections measured for a number of fibers was expressed as a percent of their value in relaxing solution in Table 2. The ratio of the $(1,1)$ and $(1,0)$ intensities is also shown as it was often taken as an index of the extent of cross-bridge binding (Haselgrove and Huxley, 1973; Brenner and Yu, 1985). Along the equator, the characteristic shift of cross-bridge mass from the myosin filament to the thin filaments was indicated by the loss of $(1,0)$ intensity as the muscle was placed in rigor solution (Fig. 7). The shift in the position of the peaks indicated shrinking of the myofilament lattice as cross-bridges bound to thin filaments. The shrinkage of the filament lattice estimated from the spacing of the $(1,0)$ and $(1,1)$ reflections was $5.1 \pm 2.3\%$ (mean $\pm$ SD). The shrinkage was less than that found by Matsubara et al., (1984), but these authors used mechanically skinned muscle fibers that were particularly swollen when relaxed. The relatively small shrinkage in the lattice spacing may also have resulted from the low force level obtained in the rigor state (Brenner and Yu, 1985). The equatorial reflections in the active pattern were intermediate between the relaxed and rigor. $I(1,1)$ decreased $(0.55 \pm 0.03$, mean $\pm$ SEM, $n = 24)$ compared to the rigor value, whereas $I(1,0)$ practically did not change (1.13 ± 0.09). The meridian was characterized by a strong reflection at 14.5 nm in relaxing solution that decreased sharply during rigorization, but recovered during activation. The 21.5-nm reflection, which is thought to arise from distortion of the 43-nm repeat of the cross-bridges, was pronounced in relaxing solution, but largely disappeared in rigor and during activation. There was a change of shape of the 14.5-nm reflection as seen in the two-dimensional picture of Fig. 6 as during activation the reflection spread along the layer line more markedly than in the relaxing solution, and the background along the meridian was also elevated as described by Lowy and Poulsen (1990). This elevation in the background could not be accounted for by the presence of CK in the activating solution or by a further shrinkage of the lattice (average change in spacing of the $(1,0)$ and $(1,1)$ reflections during activation was $3.4 \pm 1.6\%$, mean $\pm$ SD, $n = 6$).

It was found that the lattice spacing in rigor usually decreased by a further 1–2% after EDC cross-linking. The rigor lattice in cross-linked fibers was slightly less compressed than during contraction (Fig. 7). It appeared that the main determinant of lattice spacing in our experiments was the force level, rather than the chemical modification of the
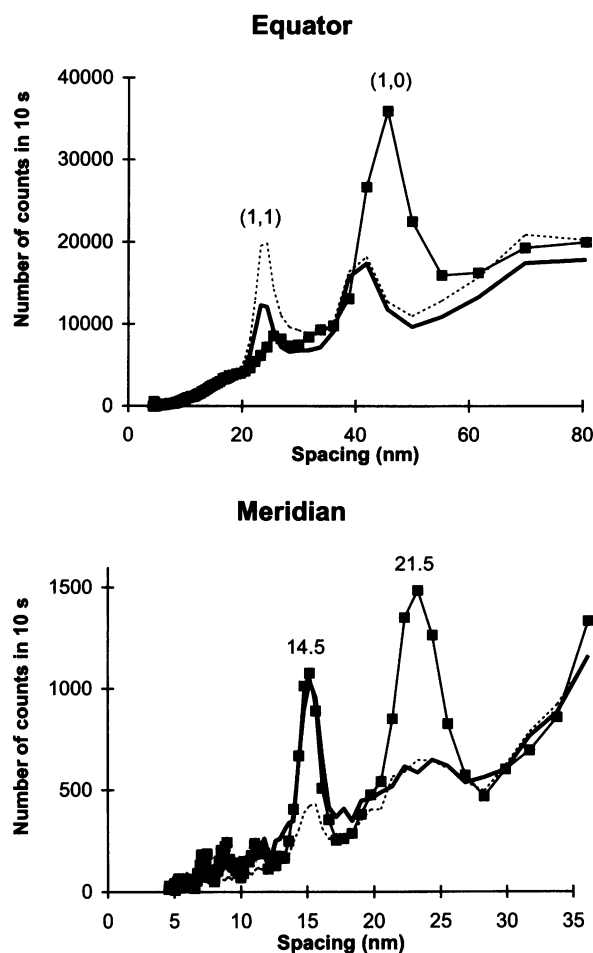

Equator

Meridian

FIGURE 7   Integration along the equator and the meridian for the data of Fig. 6, showing the change in the intensity of the reflections for the muscle fiber in the relaxed (■), rigor (- - -), and active (—) states. Only half of each symmetrical one-dimensional pattern is shown. The center of symmetry of the pattern is to the right of the figures. The number of counts is that after background subtraction as described in the Methods section. The abscissa represents the calculated reciprocal spacing, using the following values: camera length, 2.79 m; x-ray wavelength, 0.154 nm; pixel size, $0.215/256 = 8.4 \times 10^{-4}$ m where 0.215 m is the effective length of the sides of the electronic area detector. With these values, the third to twelfth orders of reflections obtained from diffraction of wet rat tail collagen correspond to their calculated spacing based on a first-order repeat of 67 nm. (Bordas et al., 1991).

muscle fiber. The rather expanded lattice observed in muscle fibers in rigor here (both before and after EDC treatment) compared with other measurements in the literature could therefore be attributed to the rigorization procedure

TABLE 2 Intensity of the main x-ray reflections (Mean ± SEM)

Conditions	n	I(145)	I(1,0)	I(1,1)	I(1,1)/I(1,0)
Relaxing solution before skinning	8	117 ± 17	100 ± 12	112 ± 10	0.25 ± 0.06
Relaxing solution after skinning	28	100	100	100	0.23 ± 0.02
Rigor	28	37 ± 4	34 ± 4	558 ± 59	4.10 ± 0.55
Rigor after EDC cross-linking	24	27 ± 4	35 ± 5	550 ± 71	3.35 ± 0.36
Active	27	98 ± 12	44 ± 6	322 ± 40	1.88 ± 0.32

used here which resulted in low force development by the rigor fibers.

The diffraction pattern in super-relaxing solution was different from that in relaxing solution before cross-linking: the intensity of the 14.5-nm meridional reflection was reduced, and the 43-nm layer line, which is very apparent in relaxing solution, was lost in the super-relaxing solution after cross-linking. The equatorial pattern appeared relaxed in super-relaxing solution, albeit not as relaxed as before cross-linking. $I(1,1)/I(1,0)$ in super-relaxing solution was 0.6 to 0.8, much less than that during active contraction (1.88, Table 2), but higher than the value of 0.25 found before cross-linking. This difference may be caused by the small number of cross-bridges that remained cross-linked to the thin filaments.

Changes in the intensity of the 14.5-nm reflection in response to changes in muscle length in rigor

We investigated the possibility of detecting structural changes in myosin cross-bridges induced by mechanical stress in rigor where the cross-bridges were strongly attached to the thin filaments. For this, a muscle fiber was cyclically stretched by 0.4% of its length in rigor and after 100 ms released back to its initial length. 100 ms after the release, the cycle was repeated again. A total of 110 cycles were applied, and the x-ray diffraction patterns in stretched and released states collected for 11 s each were compared. No significant difference in the intensities of (1,0) and (1,1) equatorial reflections was detected, whereas the intensity of the 14.5-nm meridional reflections increased by 35% (from 1546 to 2095 counts per 11 s) following the stretch.

Changes in the intensity of the 14.5-nm reflection in response to changes in muscle length during active contraction

Following the experiments of Huxley et al. (1983) with whole muscles and Irving et al. (1992) and Lombardi et al. (1995) with intact fibers, we investigated the possibility of detecting changes in cross-bridge orientation in permeabilized muscle fibers with the eventual aim of determining the role of nucleotides on the kinetics of this structural change. We applied length steps (releases and stretches) with an amplitude of 0.45% to 0.8% of the fiber length. Changes in sarcomere length determined from the signal of the position sensitive photodiode were smaller and varied from 2.5 to 5 nm/half sarcomere (4 ± 1.1, mean ± SD). A total of 478 releases and stretches were applied, using 13 partially cross-linked muscles fibers. The changes in intensity in the 14.5-nm meridional reflection are shown in Fig. 8, collected in 1-ms time bins during the rapidly changing phases, together with the sarcomere and tension signal for one length change. The time resolution of the intensity measurement was limited by the number of photons that we were able to collect. Each muscle fiber provided ~10 photons per mil-
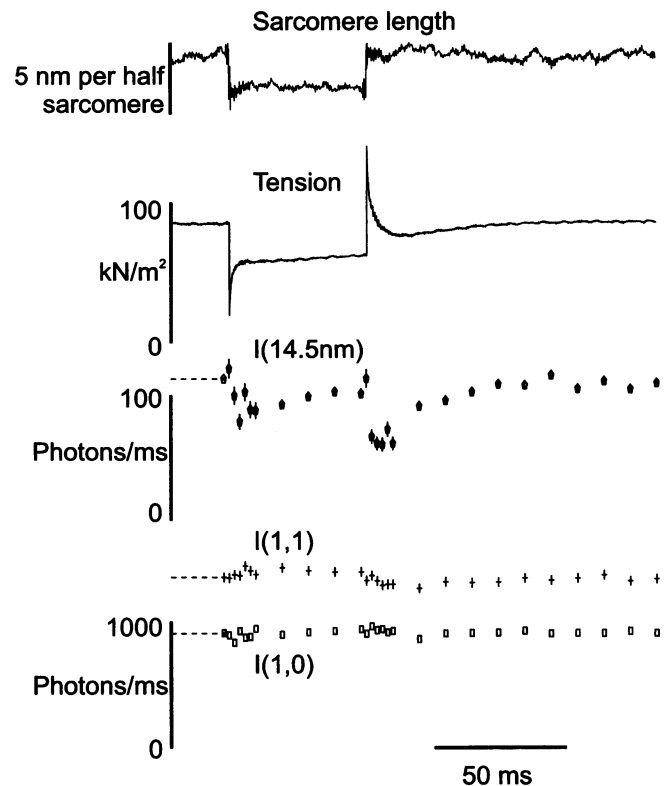

FIGURE 8 Time course of the change in the 14.5-nm meridional reflection following rapid release and stretches in activated muscle fibers at 5°C. Top and second traces are representative records of the sarcomere length and tension signals. Third trace from the top is the sum of the photons collected for a total of 478 length steps from 13 fibers. Similarly the bottom two traces represent the intensities of the (1,1) and (1,0) reflections. The dashed lines represent the intensity level, as measured in a 100 ms-long time frame, before the length step. The data were obtained by submitting partially cross-linked fibers to cycles of length changes during activation. From 10 to 60 cycles were obtained from each muscle fiber, and the photons collected for each fiber in each reflection were added for each time point.

lisecond in the 14.5-nm meridional reflection, and the data shown provided a time resolution of 2 ms.

Tension decreased during the shortening step and increased again during the rapid force recovery phase. This phase was then followed by a plateau which corresponded to phase 3 of the Huxley and Simmons (1971) transients. Tension rose instantaneously during the applied stretch, and rapidly returned to near its equilibrium value. This rapid phase was then followed by a slower increase in force reminiscent of stretch-activation seen in fibrillar muscle of the asynchronous flight muscles of some insects. The intensity of the meridional reflection decreased by 30% following the release, and then rose again to 88% of its initial value once the rapid phase of force redevelopment had ended. Following the stretch, the intensity of the meridional reflection decreased to 53% of its initial value and gradually returned to the starting value. In comparison, little change was seen in the intensity of the (1,1) and (1,0) equatorial reflections. Only a small rise in the intensity of the (1,1)

reflection was seen, which did not appear to display the transient changes seen for the meridional reflection.

DISCUSSION

We developed a procedure to obtain permeabilized frog muscle fibers that maintained the same characteristics as those in intact muscle fibers, with the added advantage of allowing experimental control of the intracellular milieu. The mechanical responses to step changes in length distinctly showed the tension phases seen in intact muscle fibers with identical kinetics. The x-ray diffraction pattern also showed that the main features were preserved, including the transitional decrease in the intensity of the 14.5-nm reflection following step releases and stretches seen in intact muscle (Huxley et al., 1983) and in single muscle fibers (Irving et al., 1992; Lombardi et al., 1995; Piazzesi et al., 1995). In addition, diffraction patterns were obtained in muscle fibers that were in the rigor state, a state difficult to achieve with intact fibers.

Extent of cross-linking

Cross-linking with EDC was used in this work as a tool for stabilizing the sarcomere structure in muscle fibers. We were concerned here with studying the properties of unlinked cross-bridges. For this reason, it was important to estimate the fraction of the cross-linked myosin cross-bridges as these may have altered mechanical and structural characteristics.

Only a fraction of the cross-bridges were cross-linked in the muscle fibers used here. This was shown by the following criteria. In super-relaxing solution that contained 50 mM BDM and 50 mM P_i and effectively detached non-linked cross-bridges from the thin filaments, tension was <10% of its active value and stiffness was 12–20% of that in rigor. The incompleteness of the slow tension recovery after fiber release by 10 nm per half-sarcomere arising from the resistance of the cross-linked cross-bridges to the filament sliding was also small (Figs. 4 and 5). As it could not be excluded that some non-cross-linked cross-bridges remained attached to the thin filaments in super-relaxing solution, it may be that the normalized stiffness provided only an upper estimate for the fraction of cross-linked cross-bridges. Also, the extensibility of actin filaments (Huxley et al., 1994; Wakabayashi et al., 1994) led to a nonlinear relationship between stiffness and the number of attached cross-bridges. The estimate of the fraction of the cross-linked cross-bridges in the experiments presented here was 10–15% if the compliance of thin filaments was taken into account (Bershitsky and Tsaturyan, 1995b).

The extent of cross-linking in the present work was less than that reported for EDC cross-linking of muscle fibers from rabbit muscle reported by Iwamoto and Podolsky (1993) for cross-linking conditions close to those used here, and similar to that found by Bershitsky and Tsaturyan (1995b), also for rabbit

fibers. The differences may be due to a difference in the measurement of the extent of cross-linking.

Mechanical transients in partially cross-linked fibers

Mechanical transients induced by the step length changes shown in Figs. 4 and 5 were similar to those in intact muscle fibers. The T_1 and T_2 curves intercepted the abscissa at 6 and 12 nm per half-sarcomere, respectively (Fig. 5 A), as in intact muscle fibers (Ford et al., 1977). The increase in the rate constant of the fast partial tension recovery with increasing amplitude of the release (Fig. 5 B) was also similar to that in intact fibers. On the other hand, it was shown earlier by Goldman and Simmons (1984, 1986) that after permeabilization, the quantitative characteristics of the mechanical transients were different from those of intact fibers: the slope of the T_1 curve decreased and the T_2 curve became more linear. These changes were accompanied by disordering of the sarcomere structure during activation of permeabilized fibers (Goldman and Simmons, 1984, 1986). Apart from changes in the lattice spacing, the reason for the change in the mechanical properties of the muscle fibers after permeabilization was heterogeneity of activation and consequently of contraction because of diffusion, not because of permeabilization itself. The data presented here show that preservation of the sarcomere structure maintained the mechanical properties.

Intensities of x-ray reflections

The x-ray diffraction patterns in partially EDC cross-linked relaxed, activated, and rigorized muscle fibers in air (Fig. 6 and Table 2) were similar to those observed in intact muscles and muscle fibers in solution. The intensities of the equatorial reflections (1,0) and (1,1) in relaxed, active, and rigor states observed here were close to those found in intact frog sartorius muscles in the resting, contracting, or rigor states (Huxley, 1968; Haselgrove and Huxley, 1973). For example these latter authors found $I(1,1)/I(1,0)$ of 0.52, 1.78, and 4.0 in the resting, contracting, and rigor states, respectively, for sartorius muscles at 4°C at a sarcomere length of 2.1 μm. These values were close to those reported here (Table 2). The lower ratio found for relaxed muscle may be a consequence of the lattice expansion observed in permeabilized muscle fibers. However, when intact frog muscles or muscle fibers were put into the rigor state by either adding iodoacetate to Ringer's solution or removing ATP from solution after permeabilization, the sarcomere structure usually disordered and the x-ray reflections became attenuated and diffuse, which made it difficult to compare intensities of the reflections with those during active contraction in a quantitative way. The loss of sarcomeric order during activation could be minimized in rabbit psoas muscles by using low temperature and low ionic strength and by allowing muscle fibers to shorten under

light isotonic loads during prolonged contractions (Brenner and Yu, 1985). Brenner and Yu (1989) obtained a value for $I(1,1)/I(1,0)$ for rigor muscle fibers similar to that obtained in this study (3.8 and 4.1, respectively), but the ratio for relaxed rabbit fibers was always greater than 1, compared with 0.25 in this study and 0.5 for intact frog sartorius muscle (Haselgrove and Huxley, 1973). This relatively high value may be a feature of relaxed rabbit muscle structure at a temperature well below its in vivo temperature.

It had not been possible previously to unequivocally ascertain whether in frog muscle fibers the loss of meridional intensity resulting from rigorization was a consequence of disordering or was the result of a change in cross-bridge orientation. Here we used BDM to avoid distortion of sarcomeres during rigorization and then fixed the sarcomere structure in rigor by slight EDC cross-linking. This enabled us to consider that the large and reversible changes in the x-ray diffraction pattern during the transition from rigor to active states were due to changes in the structure of the cross-bridges, not changes in the macroscopic order of the sarcomeres. Cross-linking itself did not appear to cause any change in the x-ray diffraction pattern of the rigor fibers. The most obvious changes during active contraction compared to rigor after cross-linking were: the disappearance of the actin-based layer lines, the increase in diffuse scattering, a twofold decrease in the intensity of equatorial reflection (1,1) with a relatively small increase in the intensity of (1,0) reflection, and a threefold increase in intensity of the 14.5-nm meridional reflection. Note this dramatic increase in the meridional intensity in the rigor to active transition was accompanied by a decrease in the number of attached cross-bridges estimated by stiffness and the ratio of the (1,0) and (1,1) equatorial intensities. This decrease in number of attached cross-bridges may account for the loss of intensity in the actin-based layer lines. The large increase in the intensity of the meridional reflection during rigor-to-activation transition could be brought about by considering that cross-bridges were more perpendicular to the fiber axis in the active than in the rigor state.

The mathematical model recently proposed by Malinchik and Yu (1995) was used to calculate the intensities of (1,0) and (1,1) equatorial reflections. We found that the intensities observed in active muscle could not be accounted for by a model where active muscle was represented by a mixture of cross-bridges either in the relaxed or rigor states. The radial position of detached myosin cross-bridges in contracting muscle was different from those in rigor and during relaxation. This suggests that the detached cross-bridges in the active fibers did not interfere with the sharp distribution of cross-bridge angles. It is therefore reasonable to consider that the detached cross-bridges in active fibers did not take up a defined orientation.

Time-resolved measurements

The decrease in the intensity of the 14.5-nm reflection in response to step changes in muscle length was greater for

stretches than for releases of the same amplitude. This corresponds to the findings of Piazzesi et al. (1995) who found that in activated, intact muscle fibers a release of 5 nm/half sarcomere and a stretch of the same amplitude resulted in intensity decreases of 27 and 48%, respectively. These values were close to our values of 30 and 47%, respectively, for similarly sized length steps. The time resolution of our experiments, similar to that obtained by Huxley et al. (1983) for whole intact muscles, was not sufficient to check if the instantaneous elastic response of the 14.5-nm intensity to the length step change (Lombardi et al., 1995) was present in our preparations.

Stretch in rigor induced an increase in the intensity of 14.5-nm meridional reflection without any significant changes in the intensities of the equatorial reflections. This suggested that at least some part of the cross-bridge elasticity was localized in the myosin cross-bridge (subfragment-1) itself and tension turned the cross-bridge or part of it into an orientation more perpendicular to the filament axis. This behavior was different from that during active contraction where both release and stretch induce a decrease in the intensity of 14.5-nm meridional reflection. Our observations agree well with the data of Irving et al. (1995) showing that the length step perturbations induced different changes in the myosin cross-bridges in rigor and during active contraction.

REFERENCES

Bershitsky, S. Y., and A. K. Tsaturyan. 1989. Effect of Joule temperature jump on tension and stiffness of permeabilized muscle fibers. *Biophys. J.* 56:809–816.

Bershitsky, S. Y., and A. K. Tsaturyan. 1992. Tension responses to Joule temperature jump in skinned rabbit muscle fibres. *J. Physiol.* 447:425–448.

Bershitsky, S. Y., and A. K. Tsaturyan. 1995a. Slight EDC cross-linking stabilizes sarcomere structure and preserves mechanical properties of permeabilized muscle fibres of the frog. *J. Physiol.* 483:76P–77P.

Bershitsky, S. Y., and A. K. Tsaturyan. 1995b. Force generation and work production by covalently cross-linked actin-myosin cross-bridges in rabbit muscle fibers. *Biophys. J.* 69:1011–1021.

Bordas, J., G. P. Diakun, J. E. Harries, R. A. Lewis, G. R. Mant, M. L. Martin-Fernandez, and E. Towns-Andrews. 1991. Two-dimensional time resolved x-ray diffraction of muscle: recent results. *Adv. Biophys.* 27:15–33.

Brenner, B., and L. C. Yu. 1985. Equatorial x-ray diffraction from single skinned rabbit psoas fibers at various degrees of activation. *Biophys. J.* 48:829–834.

Brenner, B., and L. C. Yu. 1993. Structural changes in the actomyosin cross-bridges associated with force generation. *Proc. Natl. Acad. Sci. USA.* 90:5252–5256.

Ferenczi, M. A., E. Homsher, and D. R. Trentham. 1984. The kinetics of magnesium adenosine triphosphate cleavage in skinned muscle fibres of the rabbit. *J. Physiol.* 352:575–599.

Ford, L. E., A. F. Huxley, and R. M. Simmons. 1977. Tension responses to sudden length change in stimulated frog muscle fibres near slack length. *J. Physiol.* 269:441–515.

Godt, R. E., and B. D. Lindley. 1982. Influence of temperature upon contractile activation and isometric force production in mechanically skinned muscle fibers of the frog. *J. Gen. Physiol.* 80:279–297.

Gill, S. C., and P. H. von Hippel. 1989. Calculation of protein extinction coefficients from amino acid sequence data. *Anal. Biochem.* 182: 319–326.

Goldman, Y. E., and R. M. Simmons. 1984. Control of sarcomere length in skinned muscle fibers of *Rana temporaria* during mechanical transients. *J. Physiol.* 350:497–518.

Goldman, Y. E., and R. M. Simmons. 1986. The stiffness of frog skinned muscle fibres at altered lateral filament spacing. *J. Physiol.* 378: 175–194.

Grabarek, Z., and J. Gergely. 1990. Zero-length crosslinking procedure with the use of active esters. *Anal. Biochem.* 185:131–135.

Haselgrove, J. C., and H. E. Huxley. 1973. X-ray evidence for radial cross-bridge movement and for the sliding filament model in actively contracting skeletal muscle. *J. Mol. Biol.* 77:549–568.

Huxley, A. F., and R. M. Simmons. 1971. Proposed mechanism of force generation in muscle. *Nature.* 233:533–538.

Huxley, H. E. 1968. Structural difference between resting and rigor muscle: evidence from intensity changes in the low angle equatorial x-ray diagram. *J. Mol. Biol.* 37:507–520.

Huxley, H. E. 1996. A personal view of muscle and motility mechanisms. *Ann. Rev. Physiol.* 58:1–19.

Huxley, H. E., and W. Brown. 1967. The low-angle x-ray diagram of vertebrate striated muscle and its behaviour during contraction and rigor. *J. Mol. Biol.* 30:383–434.

Huxley, H. E., A. Stewart, H. Sosa, and T. Irving. 1994. X-ray diffraction measurements of the extensibility of actin and myosin in contracting muscle. *Biophys. J.* 67:2411–2421.

Huxley, H. E., A. R. Faruqi, M. Kress, J. Bordas, and M. H. J. Koch. 1982. Time-resolved x-ray diffraction studies of the myosin layer-line reflections during muscle contraction. *J. Mol. Biol.* 158:637–684.

Huxley, H. E., R. M. Simmons, A. R. Faruqi, M. Kress, J. Bordas, and M. H. J. Koch. 1983. Changes in the x-ray reflections from contracting muscle during rapid mechanical transients and their structural implications. *J. Mol. Biol.* 169:469–501.

Irving, M., T. St. C. Allen, C. Sabido-David, J. S. Craik, B. Brandmeier, J. Kendrick-Jones, J. E. T. Corrie, D. R. Trentham, and Y. E. Goldman. 1995. Tilting of the light chain region of myosin during length step changes and active force generation in skeletal muscle. *Nature.* 375: 688–691.

Irving, M., V. Lombardi, G. Piazzesi, and M. A. Ferenczi. 1992. Myosin head movement are synchronous with the elementary force-generating process in muscle. *Nature.* 357:156–158.

Iwamoto, H., and R. J. Podolsky. 1993. Crossbridge rotation in EDC-cross-linked striated muscle fibers. *In* Mechanism of Myofilament Sliding in Muscle Contraction. H. Sugi and G. H. Pollack, editors. Plenum Press, New York. 393–407.

Leszyk, J., Z. Grabarek, J. Gergely, and H. Collins. 1990. Characterization of zero-length cross-links between rabbit skeletal muscle troponin C and

Troponin I: evidence for direct interaction between the inhibitory region of troponin I and the NH_2-terminal, regulatory domain of troponin C. *Biochemistry.* 29:299–304.

Lombardi, V., G. Piazzesi, M. A. Ferenczi, H. Thirlwell, and M. Irving. 1995. Elastic distortion of myosin heads and repriming of the working stroke in muscle. *Nature.* 374:553–555.

Lowy, J., and F. R. Poulsen. 1990. Studies of the diffuse x-ray scattering from contracting frog skeletal muscles. *Biophys. J.* 57:977–985

Matsubara, I., Y. E. Goldman, and R. M. Simmons. 1984. Changes in the lateral filament spacing of skinned muscle fibres when cross-bridges attach. *J. Mol. Biol.* 173:15–33.

Malinchik, S., and L. C. Yu. 1995. Analysis of equatorial x-ray diffraction pattern from muscle fibers: factors that affect the intensities. *Biophys. J.* 68:2023–2031.

Martin-Fernandez, M. L., and E. Towns-Andrews. 1993. Two-dimensional time-resolved x-ray diffraction studies of live isometrically contracting frog sartorius muscle. *J. Muscle Res. Cell Mot.* 14:311–324.

Nishiye, E., A. V. Somlyo, K. Török, and A. P. Somlyo. 1993. The effect of MgADP on cross-bridge kinetics: a laser flash photolysis study of guinea pig smooth muscle. *J. Physiol.* 460:247–271.

Piazzesi, G., V. Lombardi, M. A. Ferenczi, H. Thirlwell, I. Dobbie, and M. Irving. 1995. Changes in the x-ray diffraction pattern from single, intact muscle fibers produced by rapid shortening and stretch. *Biophys. J.* 68:92s–98s.

Poole, K. J. V., Rapp, G., Maeda, Y., and R. S. Goody. 1988. The time course of changes in the equatorial diffraction patterns from different muscle types on photolysis of caged-ATP. *Adv. Exp. Med. Biol.* 226: 391–404.

Rayment, I., H. M. Holden, M. Whittaker, C. B. Yohn, M. Lorenz, K. C. Holmes, and R. A. Milligan. 1993. Structure of the actin-myosin complex and its implications for muscle contraction. *Science.* 261:58–65.

Rayment, I., W. R. Rypniewski, K. Schmidt-Base, R. Smith, D. R. Tomchick, M. M. Benning, D. A. Winkelmann, G. Wesenberg, and H. M. Holden. 1993. Three-dimensional structure of myosin subfragment-1: a molecular motor. *Science.* 261:50–58.

Squire, J., and J. Harford. 1993. Time-resolved studies of cross-bridge movement: Why use X-rays? Why use fish muscle? *Adv. Exp. Med. Biol.* 332:435–448.

Tawada, K., and M. Kimura. 1986. Stiffness of carbodiimide-crosslinked glycerinated muscle fibers in rigor and relaxing solutions at high salt concentrations. *J. Muscle Res. Cell Mot.* 7:339–350.

Tawada, K., Y.-P. Huang, and Y. Emoto. 1989. Effect of ionic strength on force transients induced by flash photolysis of caged ATP in covalently crosslinked psoas muscle fibers. *In* Muscle Energetics. Alan R. Liss, Inc., New York. 37–43.

Towns-Andrews, E., A. Berry, J. Bordas, G. R. Mant, P. K. Murray, K. Roberts, I. Sumner, J. S. Worgan, and R. Lewis. 1989. Time-resolved x-ray diffraction station: x-ray optics, detectors and data acquisition. *Rev. Sci. Instrum.* 60:2346–2349.

Wakabayashi, K., Y. Sugimoto, H. Tanaka, Y. Ueno, Y. Takezawa, and Y. Amemiya. 1994. X-ray diffraction evidence for the extensibility of actin and myosin filaments during muscle contraction. *Biophys. J.* 67: 2422–2435.

Wray, J. S. 1987. Structure of relaxed myosin filaments in relation to nucleotide state in vertebrate skeletal muscle. *J. Muscle Res. Cell Mot.* 8:62a.